Yeast *Saccharomyces cerevisiae* adiponectin receptor homolog Izh2 is involved in the regulation of zinc, phospholipid and pH homeostasis

Mojca Mattiazzi Ušaj[1], Metod Prelec[1], Mojca Brložnik[1], Cecilia Primo[2], Tomaž Curk[3], Janez Ščančar[4], Lynne Yenush[2], Uroš Petrovič[1]

[1] Department of Molecular and Biomedical Sciences, Jožef Stefan Institute, Jamova 39, SI-1000 Ljubljana, Slovenia
[2] Instituto de Biología Molecular y Celular de Plantas (IBMCP), Universitat Politècnica de València-Consejo Superior de Investigaciones Científicas, Avd. de los Naranjos s/n, Valencia, Spain 46022
[3] Faculty of Computer and Information Sciences, University of Ljubljana, Večna pot 113, SI-1000 Ljubljana, Slovenia
[4] Department of Environmental Sciences, Jožef Stefan Institute, Jamova 39, SI-1000 Ljubljana, Slovenia

Abstract
The functional link between zinc homeostasis and membrane-related processes, including lipid metabolism regulation, extends from yeast to humans, and has a likely role in the pathogenesis of diabetes. The yeast Izh2 protein has been previously implicated in zinc ion homeostasis and in the regulation of lipid and phosphate metabolism, but its precise molecular function is not known. We performed a chemogenomics experiment to determine the genes conferring resistance or sensitivity to different environmental zinc concentrations. We then determined under normal, depleted and excess zinc concentrations, the genetic interactions of *IZH2* on the genome-wide level and measured changes in the transcriptome caused by deletion of *IZH2*. We found evidence for an important cellular function of the Rim101 pathway in zinc homeostasis in neutral or acidic environments, and observed that phosphatidylinositol is a source of inositol when zinc availability is limited. Comparison of our experimental profiles with published gene expression and genetic interaction profiles revealed pleiotropic functions for Izh2. We propose that Izh2 acts as an integrator of intra- and extracellular signals in providing adequate cellular responses to maintain homeostasis under different external conditions, including – but not limited to – alterations in zinc concentrations.

Introduction
Zinc is one of the essential nutrients necessary for sustaining life. Its overload in an organism is, however, toxic. Cells must therefore possess homeostatic mechanisms to ensure that intracellular zinc concentrations stay within the physiological limits, otherwise their growth and development are impaired[1]. The main mechanism for maintaining an appropriate intracellular zinc concentration in yeast *Saccharomyces cerevisiae* cells is its import via plasma membrane transporters (Zrt1/2, as well as Fet4 and Pho84 proteins) and its interchange between the cytosol and the vacuole, which is where excess zinc is predominantly stored in this organism[2], via vacuolar membrane transporters (Zrt3, Cot1 and Zrc1 proteins). Zinc is a structural or catalytic co-factor of many proteins and it is estimated that more than 10% of the proteins encoded in the human genome require zinc for their activity, zinc-finger proteins being the most abundant class among them[3]. Moreover, class I, II and IV histone deacetylases (HDACs) are Zn-dependent[4], indicating that changes in Zn concentrations exert significant effects on the expression levels of a subset of genes[5]. It has been furthermore suggested that the essential function of zinc is its antioxidant activity, which, among other effects on cellular processes, stabilizes cellular membranes[6].

The effect of zinc on membrane homeostasis occurs also through modulation of phospholipid metabolism. Zinc depletion in *S. cerevisiae* activates the Zap1 transcriptional activator, among whose target genes are *PIS1*, encoding phosphatidylinositol synthase, and *DPP1*, encoding diacylglycerol pyrophosphate phosphatase. Zn depletion thus causes an increase in phosphatidylinositol concentrations and a decrease in phosphatidylethanolamine concentrations[7, 8]. In addition, zinc depletion causes a decrease in the concentration of phosphatidic acid, thus triggering the release of Opi1 from the ER membrane and its translocation into the nucleus, where it represses expression of *CHO1,* encoding phosphatidylserine synthase, and *INO1,* encoding inositol-3-phosphate synthase, by inhibitory binding to Ino2/4 complex[7].

In humans, zinc depletion can lead to insulin production and secretion disorders, while hyperglycemia results in increased secretion and a concomitant decrease in total body zinc[9]. The connection between diabetes and zinc is complex and a clear cause and effect relationship is still unknown[9, 10]. One mechanism by which zinc affects metabolism and diabetes is the structural role of zinc in the formation of the insulin hexamer, the storage form of the hormone. Therefore, zinc is important for synthesis, storage, proper conformation and excretion of insulin from pancreatic β-cells[11]. Adiponectin is another polypeptide hormone that regulates metabolism in humans, and its deficiency is one of the main causes, defined on the molecular level, for insulin resistance, type 2 diabetes, and metabolic syndrome[12, 13]. Two adiponectin receptors from the progesterone-adiponectin receptor family (PAQR), AdipoR1 and AdipoR2, are known in humans and they have been shown to mediate the antidiabetic metabolic actions of adiponectin[14]. In yeast, structural adiponectin receptor homologues are encoded by *IZH1/2/3/4* (Implicated in Zinc Homeostasis) genes, deletions of which exert zinc-dependent mutant phenotypes and are, with the exception of *IZH3*, regulated by Zap1/zinc levels, as well as by the fatty acid-activated Oaf1/Pip2 transcription factors[15, 16]. *IZH2* and especially *IZH4* expression has been shown to be regulated also by Mga2[16], a transcriptional activator that in response to hypoxia induces expression of genes such as *OLE1*[17], which encodes the sole fatty acid desaturase in yeast. Izh2 is localized to the plasma membrane and is a putative functional homologue of adiponectin receptors since it binds osmotin, a plant homolog of adiponectin[18]. In addition, heterologous expression of human adiponectin receptors in yeast results in functional complementation of Izh2 in ion homeostasis, and their activation with adiponectin elicits a signaling cascade that includes the same signaling proteins as Izh2p overexpression, such as AMPK/Snf1[19]. Cells lacking Izh2 are resistant to the ergosterol-binding polyene antifungal compound nystatin[15] which provokes a transcriptional response similar to zinc depletion[20]. Based on these results, Izh2 was proposed to affect the sterol composition and consequently the permeability of cellular membranes[16]. Moreover, the transcriptional response to polyene antifungal compounds includes an increase in the expression of genes from the PHO pathway, which contributes to increased levels of free intracellular phosphate. These same genes were found to have increased expression in *izh2*Δ cells, suggesting a role for Izh2 also in the regulation of phosphate metabolism[15]. How these processes are linked through the molecular function of Izh2 is not well understood. However, it has been proposed that Izh2 is involved in a signal transduction cascade, which could be either zinc-mediated or independent of zinc[16]. To address these questions, we compared the effects of zinc depletion or overload and the absence of Izh2 protein in yeast on a genome-wide level.

Results

Chemogenetic interactions of zinc depletion and overload

In order to obtain a broad and genome-wide insight into the effects of zinc depletion and overload on yeast cells, we first performed chemogenomic analysis to identify single gene deletion strains that are sensitive or resistant, compared to the reference strain, to altered zinc concentrations[21]. For zinc depletion conditions, 50 nM $ZnCl_2$ was selected based on the semi-inhibitory effect of this concentration on the growth of the reference strain. Zinc overload conditions were achieved using 4 mM $ZnCl_2$, and 10

μM zinc was used for the control media, which is within the range found to be optimal for yeast cells[22]. The collected results are shown in Supplementary Table 1.

Three deletion strains were found to be significantly sensitive to zinc depletion. As expected, cells lacking the *ZRT1* gene, which encodes the high-affinity zinc transporter and is responsible for the majority of zinc uptake[23], were sensitive to zinc depletion. Additionally, the strain lacking the *ADH4* gene, coding for the zinc-dependent alcohol dehydrogenase isoenzyme, and the strain lacking the *TSA1* gene, encoding thioredoxin peroxidase, were found to be sensitive. Expression of *ZRT1*, *ADH4* and *TSA1* has been found to be induced in response to zinc deficiency by the Zap1 transcription factor, and *zrt1*Δ, *adh4*Δ and *tsa1*Δ strains have previously been identified as being sensitive to zinc deficiency[23-27]. These results thus provided a positive control for the zinc depletion conditions employed here, and suggested that Zap1 is the major regulator of the genes identified in the screening.

Interestingly, under conditions of zinc depletion, we identified more resistant than sensitive strains: 27 significantly resistant strains, of which 22 highly significant, were identified (Supplementary Table 1). Two mutants have known defects in ion homeostasis, *vph1*Δ and *mmt2*Δ; Vph1 is the subunit a of the vacuolar ATPase (V-ATPase) V_0 domain, and Mmt2 is a putative metal transporter[28, 29]. Three of the resistant strains had deletions of genes which participate in lipid metabolism or membrane biology-related processes: *CEM1*, encoding a beta-keto-acyl synthase with potential role in fatty acid synthesis in mitochondria[30, 31], *ATG2*, coding for a membrane protein required for vesicle formation during autophagy and pexophagy[32, 33], and *INO1*, an essential gene in environments lacking inositol, coding for inositol-3-phosphate synthase, the rate limiting enzyme for the synthesis of inositol and consequently for inositol-containing phospholipids[34, 35]. Interestingly from the perspective of zinc deficiency-related oxidative stress, the strain without the *TRR2* gene, coding for mitochondrial thioredoxin reductase, was found to be resistant to zinc depletion.

In the screening with high zinc concentrations (zinc overload), 161 strains were found to be significantly sensitive (Supplementary Table 1). As expected, the *zrc1*Δ strain lacking the transporter responsible for zinc uptake into vacuoles[22] was identified in this screening: the role of Zrc1 is to prevent acute accumulation of cytosolic zinc[36]. Also expected was a highly enriched group of genes annotated to vesicle-mediated transport (p-value=3.34e-12; http://go.princeton.edu/cgi-bin/GOTermFinder), which is a general indicator of cellular stress[37]. The strain lacking Vph1 was found to be sensitive to excess zinc – this same strain was resistant to depleted zinc (see above), suggesting that deletion of *VPH1* gene results in increased cytosolic zinc concentrations under conditions of both elevated and decreased environmental zinc concentrations. This is in agreement with the finding that V-ATPase activity is required for vacuolar zinc sequestration[38]. Another deletion strain, *ypr170c*Δ, was found to be both resistant to zinc depletion and sensitive to excess zinc. *YPR170C* is a dubious open reading frame which does not overlap any known protein coding sequence, but whose mutation leads to significantly altered phenotypes, including resistance to $ZnCl_2$ and to V-ATPase inhibitor concanamycin A[39]. The similarity between the sets of strains resistant to zinc depletion and sensitive to zinc overload extended to genes involved in autophagy and in maintenance of cellular integrity: while deletion of *ATG2*, which results in resistance to zinc depletion (see above) was not found to also cause sensitivity to excess zinc, a number of other genes involved in autophagy were found in this screening – *ATG21*, *CCZ1*, *MON1*, *TRS85*, *UTH1*, *VAM3*, *VAM6*, *VAM7*, *VPS41*, *VTC1*, *VTC4* and *YPT7.* The majority of these genes is also involved in membrane invagination. These two biological process ontology classes were among the enriched ones (p-value=1.8e-4 for membrane invagination and p-value=2.29e-3 for autophagy) among the hits sensitive to excess zinc. Deletion of the *MGA2* gene, encoding the ER membrane-bound protein involved in the activation of the expression of *OLE1* transcription (see above), also resulted in increased sensitivity to zinc overload.

Ninety-seven strains were found to be resistant to excess zinc relative to wild-type growth (Supplementary Table 1). No overlap was found with the strains sensitive to zinc depletion, indicating

that no single gene deletion results in permanently lower intracellular zinc concentrations. Two strains, *slm3*Δ and *yll056c*Δ, were however identified as resistant to both high and low zinc concentrations. *SLM3* encodes a mitochondrially-localized tRNA-specific 2-thiouridylase[40], and *YLL056C* is co-expressed with genes involved in pleiotropic drug resistance[41]. Further research is necessary to elucidate the molecular mechanism behind the observed phenotypes, e.g. to establish whether the Yll056c protein is involved in zinc transmembrane transport. Strains with deletions of 5 genes, *CTI6*, *DEP1*, *RXT2*, *SIN3* and *UME1*, encoding components of Rpd3L histone deacetylase complex, were found in the excess zinc-resistant group as well. The Rpd3L complex represses transcription of its target genes through the activity of the Rpd3 deacetylase. In this group is also the *dep1*Δ strain that had the highest observed relative resistance. Importantly, the *dep1Δ* mutant has previously been found to be unable to regulate expression of *INO1* and *CHO1* genes[42]. Also, Sin3 has been previously shown to regulate the expression of *OPI1* gene[43], whose product regulates expression of *INO1* and *CHO1* (see above).

The next group of functionally related genes whose deletions resulted in increased resistance to zinc overload consists of *DFG16*, *RIM9*, *RIM20* and *RIM101*. These genes code for key components of the Rim101 pathway which is important for the adaptation of cells to alkaline pH[44]. One additional gene whose mutation led to resistance to excess zinc, *YGR122W*, has been implicated in Rim101 activation[45]. Since additional genes encode factors important for the Rim101 pathway[46], we decided to determine the relative sensitivity to excess zinc of single deletion mutants of all known components of the pathway (Table 1). Phenotypes of the mutants identified in the screening were confirmed, and additionally deletions of genes *VPS28*, *RIM8*, *RIM13*, *RIM21* and *SNF7* were shown to confer resistance to excess zinc as well. Therefore, genetic perturbations of all components involved in the signal transduction from the plasma membrane to the endosome at high pH[47] were shown to result in resistance to zinc overload.

Combinatorial effects of pH, excess zinc and Rim101 pathway inhibitions

To elucidate in more detail how cellular responses to high pH and elevated zinc concentrations are connected, we determined growth rates under conditions of different pH and elevated zinc levels, in the reference strain and in strains lacking *RIM101*, encoding the transcription factor that represents the last step of the Rim101 signaling pathway[48], *RIM20*, encoding the activator of Rim101 protein[49], or *RIM9*, encoding a protein functioning at the early/detection step of this signaling pathway[50] (Figure 1A-C). Cells were grown in liquid media at pH 4 or 6 (higher pH values could not be used due to zinc precipitation), and with either 2.5 μM zinc (control concentration), or supplemented with 2 mM or 4 mM zinc (zinc overload). This experiment showed that the reference strain is more resistant to elevated zinc at higher pH, as the cells grew significantly better in the presence of 2 mM zinc at pH 6 than at pH 4. Deletion of any of the three *RIM* genes tested increased the resistance to zinc at pH 6, but even more significantly at pH 4. A similar, although significantly less pronounced effect was also observed in the *zap1Δ* strain (Figure 1D). These results suggest that cellular responses triggered by the Rim101 pathway have a negative effect on the adaptation to elevated zinc.

Genetic interactions of IZH2

Synthetic genetic array technology[51] was used to generate double deletion mutant strains in the *izh2*Δ background. Genetic interactions of *IZH2* were then determined in the presence of decreased, normal and increased zinc concentrations (Supplementary Table 2). Altogether, 204 genes showed a negative genetic interaction with *IZH2* (Figure 2A). Of these, 5 genes were found under all three conditions, while an additional 16 were identified as interactors under two conditions (Supplementary Table 2). We could not find any clear functional links between these genes. The remaining genes were found only under a single condition.

Thirty-two genes found to genetically interact with *IZH2* code for proteins that are localized to membranes. Products of eight of them (*AAC1*, *BAP3*, *BOR1*, *MEP1*, *MIR1*, *MRS2*, *STV1* and *TIM18*), exert

transmembrane transport activity; interestingly, five are mitochondrial. Stv1 is one of the two isoforms of the subunit a of the V-ATPase V_0 domain[52]; the other isoform is Vph1, and the *vph1Δ* strain was found to be sensitive to excess zinc and resistant to depleted zinc (see above). In addition, *RAV1* was found to genetically interact with *IZH2*; Rav1 promotes assembly of the V-ATPase holoenzyme[53, 54]. These results are in agreement with the finding that *izh2Δ* strain is sensitive to elevated zinc concentrations[16, 55], a condition that requires vacuolar zinc sequestration. Previous studies[55, 56] have identified 11 genes which show a negative genetic interaction with *IZH2*. Two of these, *ENV9* and *EOS1*, were also found in our study, and Env9 has also been found to be involved in vacuolar functions[57]. On the other hand, Izh2 was shown to suppress the hydrogen peroxide-sensitive *EOS1* mutation, indicating a role for Izh2 in oxidative stress response[55]. Gene Ontology annotation enrichment analysis did not identify any significantly ($p<0.01$) enriched functional classes in the set of genes which interact genetically with *IZH2*, and the most enriched biological process was 'regulation of RNA metabolic process' (p-value=0.052).

Comparison of the genetic interactions and the zinc depletion/overload chemogenomics screening showed that 25 genes display both genetic interaction with *IZH2* and significantly altered sensitivity/resistance to zinc (Figure 2B). This number is higher than expected by chance only (p-value= 0.00115). The group of 15 genes which show a negative genetic interaction with *IZH2* and whose deletion strains are at the same time sensitive to excess zinc is enriched for genes involved in vacuolar transport, as it includes *VPS9*, *VPS55* and *VTC1*. Two of these genes were found to genetically interact with *IZH2* specifically at elevated zinc: *VPS55*, a late endosomal protein and a functional homolog of human leptin receptor overlapping transcript protein (LEPTOR)[58], and *VTC1*, a subunit of the vacuolar transporter chaperone complex which is also involved in vacuolar polyphosphate accumulation and has mRNA binding activity[59-61]. In the group of 9 genes in negative genetic interaction with *IZH2* whose deletion strains are at the same time resistant to excess zinc there are several genes that regulate cellular physiology. Genes encoding proteins involved in chromatin modification, *UME1* and *IOC4*, as well as the *SKN7* gene, encoding a transcription factor, were found to genetically interact with *IZH2* under conditions of zinc deficiency, whereas genes encoding two other transcription factors/transcriptional regulators (Xbp1 and Tos9), and two protein kinases (Ptk2 and Sak1) were found to be in genetic interaction with *IZH2* at normal zinc concentrations. These differences imply that Izh2 has multiple roles in the cell under different environmental zinc concentrations.

Effect of IZH2 deletion on gene expression

To further analyze the role of Izh2 in yeast cells, we compared gene expression in *izh2*Δ and reference strains, under conditions of normal (10 μM) and limiting (50 nm) zinc concentrations. To assess the role of Izh2 globally, results from normal and limiting zinc were combined to minimize the effect of environmental conditions and to increase statistical significance. To investigate the specific function of Izh2 under different conditions, the results were analyzed separately, but these results are statistically less robust. The expression results are presented in Supplementary Table 3 and available from the ArrayExpress database under the accession number E-MEXP-3995.

First, we were interested in genes with decreased expression in *izh2*Δ cells under any condition, since this group should contain genes whose expression is potentially activated by Izh2. The most significantly down-regulated gene was *VEL1*, encoding a protein with unknown function. *VEL1* has been identified as a gene with highly induced expression in zinc-depleted conditions in a Zap1-dependent manner[62]. Also in our experiments the decrease in expression was more pronounced at low zinc concentrations, suggesting that besides Zap1, Izh2 is required for the induction of *VEL1* expression. The physiological role of this effect is however currently not known. To gain insight into the physiological consequences of *IZH2* deletion, we performed functional enrichment analysis (http://go.princeton.edu/cgi-bin/GOTermFinder) on genes with decreased expression in *izh2*Δ cells (Supplementary Table 3, $p<0.01$). The most significantly enriched were processes related to iron homeostasis (e.g. biological process 'iron

chelate transport' with the p-value=5.7 × 10^{-4}) and included genes *FIT1*, *FIT2*, *FIT3*, encoding glycosylphosphatidylinositol (GPI)-anchored mannoproteins involved in the retention of siderophore-iron in the cell wall[63], *FET4*, encoding an importer for iron, zinc and copper, and *MCD4*, encoding an evolutionarily conserved protein involved in GPI anchor biosynthesis. We also specifically looked at genes involved in lipid metabolism and found several with decreased expression in *izh2*Δ cells: *INO1*, *CHO1*, *TSC10* (encoding 3-ketosphinganine reductase, an essential enzyme in phytosphingosine synthesis), *ERG28* (encoding an ER membrane protein involved in ergosterol biosynthesis), *APQ12* (a gene with synthetic lethal genetic interactions with genes involved in lipid metabolism, encoding for a protein required for nuclear envelope morphology), and, again, *MCD4*. Among the genes with decreased expression in *izh2*Δ cells was also *CLN3*, encoding a G1 cyclin which, unlike other cyclins, is not regulated by the cell cycle, but is instead under the control of nutrient repletion by acetyl-CoA-mediated chromatin modification[64]. One of the few genes with decreased expression in *izh2*Δ cells under normal zinc conditions only was *ZRT1*.

In the group of genes with induced expression in *izh2*Δ cells, the most significantly enriched group contained genes involved in polyphosphate metabolism or phosphate transport (e.g. biological processes 'polyphosphate metabolic process' with the p-value=1.3 × 10^{-5}, 'phosphate ion transport' with the p-value=3.9 × 10^{-4} and 'phosphorus metabolic process' with the p-value=4.3 × 10^{-4}). In this group are genes encoding acid phosphatases (*PHO3*, *PHO5*, *PHO11* and *PHO12*) and phosphate transporters (*PHO84*, *PHO89* and *PIC2*), as well as *SPL2*, encoding a protein similar to cyclin-dependent kinase inhibitors that negatively regulates low-affinity phosphate transport in low phosphate environments[65, 66], and *VTC4* and *VTC1*.

Determination of changes in the transcriptome upon gene silencing is a powerful approach for functional characterization of genes[67, 68]. Profiles obtained with such approaches represent a fingerprint of the effects a gene has on cellular physiology[69]. For a multifunctional protein, genome-wide expression profiles of the deletion mutant should reflect the different cellular pathways affected by the absence of the respective gene/protein. The set of 67 identified genes that change their expression in response to the absence of Izh2 more than 2-fold under conditions of zinc depletion overlaps significantly (29 genes; hypergeometric distribution p=3.68 × 10^{-27}) with the 185 genes that have been found as differentially expressed in *zap1Δ* cells shifted to low zinc environment[70]. Less significant overlap (21 genes; p=1.1 × 10^{-3}) exists with the 1001 differentially expressed genes of cells which have been for 6 hours depleted for H4 histone[71]. This suggests that some genes that are regulated by a decrease in zinc concentration, but not by Zap1, are under the control of Izh2, and indicate that the effect of Izh2 on gene expression is perhaps at least partly the result of chromatin modification/remodeling. Based on this expression patterns comparison we compiled a set of genes whose expression is changed upon decreased zinc concentration and apparently activated by Izh2, but not by Zap1 – these genes are *CLB1, ENB1, FIT1, MET6, SAG1, SRP101, TPA1* and *TSR1*. Products of two of these, *FIT1* and *ENB1*, are involved in the maintenance of iron homeostasis.

The relationship between Ino1/inositol and Zap1

Following the identification in the chemogenomic screening of the *ino1Δ* strain as being resistant to zinc depletion and in addition *INO1* gene expression being affected by Izh2, we analyzed in more detail the requirement for inositol under conditions of zinc depletion. We used liquid media without inositol, with 2 mg/mL (i.e. normal yeast medium concentration) or 20 mg/mL of inositol (excess inositol), with either 50 nM (depletion) or 2.5 µM (control) zinc concentrations, and determined the growth rates of the wild-type, *ino1*Δ and *zap1*Δ strains. To minimize the effect of residual Zn and inositol in the cells, pre-cultures were grown in medium with 2 mg/mL inositol and 50 nM Zn. Reference strain cells grew slower in media with lower inositol concentrations under zinc depletion, but were not affected by the lack of inositol under normal zinc conditions (Figure 3A-B). These results suggest that adaptation to low zinc

concentrations requires higher amounts of inositol, and/or that cellular adaptation to decreased levels of zinc hinders inositol biosynthesis. The former notion is supported by faster growth of all three tested strains with elevated 20 mg/mL inositol concentrations under zinc depletion (Figure 3C). The latter notion could be caused by inhibition of Ino1, the key enzyme in inositol biosynthesis, under zinc depletion, in agreement with the findings that under such conditions Opi1 is released from the membrane and translocated into the nucleus[7]. Consistent with this possibility, we observed a small relative decrease in the growth rate of *ino1*Δ cells grown in depleted zinc in the presence of 2 mg/mL inositol, compared to that of the reference strain. Interestingly, we observed a partial rescue of *ino1*Δ cells in medium lacking inositol by zinc depletion. We assume that this occurs because of elevated PI content under low zinc conditions, caused by Zap1 activity and PI being an important source of inositol even in cells with active Ino1[7, 72]. Growth of *zap1Δ* cells, as expected, was decreased at low Zn concentrations, and additional inositol depletion significantly potentiated this trend (Figure 3). This result is in line with the assumption that PI serves as a source of inositol, as well as with the possibility of Zap1 being involved in the regulation of *INO1* gene expression, possibly indirectly through altered PI levels and Opi1 activation[72].

The role of the Zrt1 transporter

Given the fact that expression of *ZRT1* has been reported to be regulated by Rim101[73], in addition to regulation by Zap1[2723], and according to our data also by Izh2 (see above), we investigated in more detail the role of Zrt1 in the increased resistance of Rim101 pathway component deletion strains to elevated environmental zinc concentrations. Protein abundance of Zrt1-GFP was measured in *rim101*Δ, *rim8*Δ and the corresponding wild type reference strain under normal zinc concentrations, at elevated zinc concentrations (2 mM; Figure 4A), or after the treatment with the EDTA chelator causing zinc depletion (Figure 4B). We found elevated levels of Zrt1 in the Rim101 pathway mutants under normal zinc conditions, in agreement with the findings from Hu and coworkers[73], and also under elevated zinc conditions (Figure 4A). Rapid increase of Zrt1 expression occurs upon zinc depletion with EDTA, and this process is unaffected in the mutants of the Rim101 pathway (Figure 4B). The latter effect was also followed on *ZRT1* gene expression level by Northern blot. We observed a slight, but reproducible and significant increase in *ZRT1* mRNA accumulation under normal growth conditions in the Rim101 pathway mutants, consistent with the increase in Zrt1-GFP observed under the same conditions, and a strong increase of *ZRT1* mRNA accumulation upon EDTA treatment in all three strains, but more rapidly in *rim101*Δ (Figure 4C). The relative amount and subcellular localization of Zrt1-GFP was also determined in the three strains under the same experimental conditions by confocal microscopy. In all cases, the relative Zrt1-GFP abundance observed in the immunoblots was confirmed and Zrt1-GFP was always localized to the ER and the plasma membrane (data not shown), in agreement with previous reports (yeastgenome.org: YPL+, YeastGFP).

The increased amount of Zrt1 cannot *per se* explain the resistance of the Rim101 pathway deficient mutants to elevated environmental zinc concentration. We reasoned that Rim101 pathway mutants might have for some reason lower intracellular zinc levels, despite higher expression of Zrt1. We therefore measured the intracellular zinc concentrations under normal and elevated environmental zinc levels in *rim101*Δ, *rim8*Δ, *dfg16*Δ, *zrt1*Δ, *zap1*Δ and the corresponding wild type reference strain. Contrary to our hypothesis, total intracellular zinc concentration in the Rim101 pathway mutants was indistinguishable from the reference wild type strain under normal environmental zinc, and, if anything, slightly increased when 4 mM $ZnCl_2$ was added to the medium (Figure 5A&B). Very similar results were obtained also for the *zrt1*Δ strain, whereas in the *zap1*Δ strain intracellular zinc concentration was significantly lower in an environment with normal zinc concentrations, but slightly exceeded the wild type levels when 4 mM $ZnCl_2$ was added to the medium (Figure 5A&B). Notably, as described previously, Rim101 pathway component deletion strains have increased resistance to zinc overload in the

environment, despite the fact that their total intracellular zinc concentrations are comparable to that of the wild type strain (Figure 5C). These findings therefore further suggest that active Rim101 pathway causes some cellular effects which decrease the resistance to zinc toxicity.

Discussion

Adaptation to extreme zinc concentrations is a complex cellular process that affects several biochemical pathways. The first line of adaptation has to provide adequate concentrations of zinc in the cytosol and this is achieved by increased uptake rate from the environment or release from the vacuole in case of zinc depletion, or sequestration in vacuoles in the case of excess cytosolic zinc[2]. We found in our screenings that the activity of Vph1, the subunit a of V-ATPase, is of critical importance for maintaining cytosolic zinc concentrations within the homeostatic limits, in agreement with and extending previous knowledge on the importance of the V-ATPase holoenzyme in maintaining zinc homeostasis[38]. We identified genetic interactions between *IZH2* and *STV1*, which encodes the other isomer of subunit a of V-ATPase that is however found in the Golgi apparatus and in endosomes rather than on the vacuolar membrane like Vph1[52], and between *IZH2* and *RAV1*, which encodes a subunit of the RAVE complex that facilitates assembly of the V-ATPase holoenzyme[53, 54]. These results indicate a functional link between Izh2 and the V-ATPase, which is most probably the consequence of the roles of V-ATPase and Izh2 in maintaining zinc homeostasis, as exemplified by the sensitivity of the *izh2Δ* strain to elevated zinc concentrations[16, 55].

A crucial part of cellular adaptation to decreased zinc levels is the response at the gene expression level, mostly mediated by the Zap1 transcriptional activator[27]. Our results demonstrated that Izh2 is also involved in the response to altered zinc availability at the level of gene expression regulation. We identified genes that are exclusively under the control of Izh2 and not Zap1, but we also observed some overlap between the activities of these two proteins. An example of the latter is expression of *ZRT1* gene, which is regulated by Zap1 when zinc is depleted[27], whereas our experiments revealed that it is regulated by Izh2 under normal zinc concentrations. Moreover, we showed that Izh2 regulates the expression of three genes coding for three out of four known plasma membrane transporters of zinc: Izh2 activates the expression of *ZRT1*, encoding the major, high-affinity zinc transporter, and *FET4*, encoding a low-affinity iron transporter capable of transporting zinc ions, but inhibits the expression of *PHO84*, which codes for a high-affinity inorganic phosphate transporter that also can mediate transport of zinc. Only *ZRT2*, the low-affinity plasma membrane zinc transporter, which is regulated by Zap1[27, 74], was not found to be under control of Izh2. While this transcriptional regulation by Izh2 influences zinc homeostasis, it is also important for the homeostasis of iron and phosphate. Indeed, our transcriptomic analysis revealed that Izh2 regulates expression of genes encoding additional proteins involved in iron transport and inhibits inorganic phosphate uptake by inhibiting the expression of genes coding for acid phosphatases, phosphate transporters, proteins required for vacuolar polyphosphate accumulation, and a negative regulator of low-affinity phosphate transport. These results are in agreement with and extend the results of the study by Karpichev and co-workers[15], wherein they showed that acid phosphatase activity is constitutively expressed in *izh2Δ* cells, leading to increased accumulation of polyphosphate in the mutant.

Zinc homeostasis is closely linked to regulation of phospholipid metabolism[7]. Results of our study indicate that Izh2 is connected to the phospholipid metabolism through co-regulation of the expression of *INO1* and *CHO1* genes with Zap1, strengthening also the zinc-phospholipid metabolism homeostasis connection through inositol. Based on our results, biosynthesis of inositol through Ino1 may not be beneficial for growth at low zinc concentrations, as indicated by the relative resistance of *ino1Δ* cells to zinc depletion. On the other hand, inositol biosynthesis is very likely required at high zinc concentrations where the PI concentration cannot be increased through Zap1-mediated Pis1 and Dpp1 activation. Regulation of inositol biosynthesis is also tightly linked to intracellular pH control[75]. Because of extensive

chemogenetic interactions found in this study between zinc and the Rim101 pathway components, which relay information on increased pH, we investigated the role of this pathway in zinc homeostasis in more detail. The Rim101 pathway, however, was found to have alkaline pH-independent activity that is important for zinc homeostasis. This role of the Rim101 pathway could be connected to its role in alkali cation homeostasis[76, 77], and/or be the consequence of Rim101 being a zinc-finger transcription factor. Interestingly, Rim101 represses the expression of the Nrg1 transcription factor[48], which is negatively regulated also by Izh2[19]. Since Rim101 also regulates *ZRT1* expression[73], we made a series of experiments to test whether a decrease of zinc import via Zrt1 is in any way involved in the increased resistance to zinc overload toxicity in the Rim101 pathway deficient mutants. All the obtained experimental data disputed this hypothesis, but rather provided evidence that Zrt1 responds to zinc depletion independently from the Rim101 pathway. Our results strongly suggest that the active Rim101 pathway causes cellular effects which decrease the resistance to zinc toxicity. Further studies will be needed to address this question in more detail.

Taken together, data obtained in this study indicate a multi-factorial fingerprint of Izh2. It has been known prior to our study that Izh2 plays a role in several different cellular processes, of which zinc homoeostasis has been deemed the most important, and that its activity is regulated by different input stimuli, including fatty acids and hypoxia[16, 17]. We have shown that even when a single input – change in zinc concentration – is used, Izh2 still affects several cellular processes. While for all of them a link to zinc homeostasis can be inferred, they do not necessarily affect cytosolic zinc concentrations. The results support the notion that the roles that Izh2 plays in yeast cells with sub- or super-optimal Zn concentrations are not exclusively directly linked to zinc homeostasis; actually, since Izh2 regulates expression of iron transporters and phosphatase activity, in addition to *ZRT1* expression at normal zinc concentrations, it is possible that one of its roles is to maintain the physiological ratio between intracellular zinc, iron and phosphate. A recent study revealed a similar parallel action of the major iron-regulated transcription factor, Aft1, and the Rim101 pathway[78].

Since different cellular perturbations, such as zinc content, lipid composition and hypoxia, influence the expression and activity of Izh2, and as a range of different cellular processes are apparently affected by Izh2, we propose that Izh2 functions as an integrator of intra- and extracellular signals in providing adequate cellular responses to maintain homeostasis under different perturbations. Izh2 is not the central regulator of zinc homeostasis like Zap1. It rather represents the second line of cellular adaptation to perturbations to zinc homeostasis, which complements the activity of Zap1, and, maybe even more importantly, ameliorates intracellular imbalances caused by the first line of adaptation whose primary aim is to retain a single parameter – zinc concentration in this case – within homeostatic boundaries. Izh2 thus affects a wide range of cellular processes, reflecting the multiple effects caused by changes in zinc concentration affecting the many zinc-dependent proteins. Perhaps rectifying intracellular imbalances caused by the first line of adaptation has also been the main evolutionary driver that led to multifunctionality, at least in the case of proteins involved in zinc homeostasis in yeast. For instance, Zap1-mediated regulation of *INO1*, indirectly through altered PI levels and Opi1 activation[72], is an illustration of a strategy where pathway buffering minimizes the negative effects of the action of the first line of adaptation: low zinc requires activation of zinc transporters (e.g. Zrt1) with Zap1, but zinc depletion by many Zn-dependent proteins with important roles in lipid metabolism also modulates lipid homeostasis. Zap1 therefore evolved to activate expression of *PIS1*, *CKI1* and *EKI1*, encoding key enzymes in phospholipid biosynthesis, thus co-regulating lipid metabolism. It is notable in this respect that lipid metabolism is strongly regulated at the epigenetic level[79], which is, through Zn-dependent HDACs, heavily dependent on zinc concentration. A similar hierarchy of shared control between regulators has been proposed before, for instance in membrane alterations caused by ergosterol and heme depletion[80]. While Hog1 has been the multifunctional protein shown in that study to confer cellular adaptation, it is interesting that Izh2 has been linked with both ergosterol metabolism and

cellular response to hypoxia[16, 55]. Additional overlap between hypoxia and Izh2 has been revealed in a study that demonstrated how inositol supplementation affected the yeast transcriptome such that six distinct expression responses (i.e. sub-profiles) could be identified, one of them being regulated by Mga2 and consisting of lipid-remodeling genes, including *IZH2*[81].

How does Izh2 influence gene expression? It has previously been shown that the signal transduction pathway downstream of Izh2 requires cAMP-dependent kinase and AMP-dependent kinase activities[19]. It has also been proposed that Izh2 influences the activity of Nrg1/Nrg2 and Msn2/Msn4 transcription factors[19]. In addition, the observed overlap of transcriptional profiles indicates that chromatin remodeling could be part of the Izh2-mediated signal transduction pathway. Genetic interactions found in this study between *IZH2* and genes *UME1* and *IOC4* coding for proteins involved in chromatin remodeling support this hypothesis. Moreover, majority of yeast HDACs, including Rpd3, are Zn-dependent. In our chemogenomic screening, deletions of five genes encoding components of the Rpd3L HDAC complex resulted in increased resistance to excess zinc. This is most likely a consequence of the modulation of Rpd3L complex activity by altered cytosolic zinc concentrations, which itself is regulated by Rpd3, creating a feed-back loop. Moreover, among its targets, Rpd3 has been shown to repress the expression of *ZRT3*, encoding a vacuolar transporter which releases zinc from the vacuole when this mineral is deficient[82]. Genetic and functional interactions between *UME1* and *IZH2* suggest that Izh2 could play a role in the HDAC/Zn homeostasis cross-talk, in agreement with a previously published report[24]. A possible explanation for these results is that excess zinc, which is probably a rare stressful condition in natural environments of *S. cerevisiae*, strongly activates the Rpd3L HDAC complex. It will be interesting to test in the future if, through the inhibitory effect of Dep1 on *INO1* and *CHO1* expression[42], and of Sin3 on *OPI1* expression[43], also increased zinc concentrations lead to inositol imbalance. Another link between inositol and HDACs has been revealed recently in a study which has shown that activity of class I HDACs, of which Rpd3 is a member, is regulated by inositol phosphates[83]. This finding opens the question of whether inositol biosynthesis is of central importance and highly regulated on the transcriptional level[81] due to this regulatory role, rather than because of its structural role as a part of membrane lipids. In line with the former notion, another recent study demonstrated that Kcs1, a yeast inositol pyrophosphate kinase, controls *INO1* transcription in an Opi1-independent manner, by regulating the synthesis of inositol pyrophosphates[84].

Izh2 is a homolog of AdipoR, which plays an important role in type 2 diabetes. Lipid metabolism and zinc homeostasis are unbalanced in type 2 diabetes, and the role of Izh2 in yeast elucidated here could help better understand also the role of AdipoR in human health and disease. Finally, it should be pointed out that three other IZH paralogs are present in the yeast genome, and that their role, which was not analyzed in the present study, should not be neglected, especially in the case of *IZH4,* which is similar to *IZH2* in many aspects. Further studies will be required to reveal the concerted action of Izh1, Izh2, Izh3 and Izh4 in maintaining zinc homeostasis and other biological processes that they affect.

Materials and Methods

Yeast strains, plasmids and media

To test the effect of different zinc concentrations on a genome-wide scale, the yeast *S. cerevisiae* deletion collection (*MATa his3Δ leu2Δ ura3Δ met15Δ yyyΔ::kanMX*) was used. Unless otherwise noted, individual strains from the same collection, as well as the corresponding reference strain (*MATa leu2Δ ura3Δ met15Δ his3Δ::kanMX*) were used in other experiments as described.

To integrate the GFP coding sequence at the C-terminus of *ZRT1*, the GFP::*HIS3* module was amplified by PCR from the pFA6a-GFP(S65T)-HIS3MX6 vector[85] using chimeric primers containing 20 bp corresponding to the GFP::*HIS3* module and 45 bp corresponding to the *ZRT1* sequence immediately upstream and downstream of the STOP codon required for correct recombination. Recombinants were confirmed by sequencing PCR products which were amplified from genomic DNA using a forward primer

50 bp upstream of the *ZRT1* STOP codon and a reverse primer 100 bp downstream of the *HIS3* start codon.

Chelated Yeast Casamino Dextrose (CYCD) (0.5 % (w/v) yeast nitrogen base without amino acids, divalent ions and phosphate (MP Biomedicals, USA), 0.5 % (w/v) casamino acids (Difco, USA), 0.01 % (w/v) adenine (Serva, Germany), 0.01 % (w/v) uracil (Serva, Germany), 0.01 % (w/v) tryptophan (Fluka, Germany), 2 % (w/v) glucose (Fluka, Germany), 2 % (w/v) agar (Sigma-Aldrich, USA)) was used in experiments where the effect of zinc depletion was assessed. Zinc was removed from the medium by pretreatment with Chelex 100 resin (Sigma, USA) as per manufacturer's instructions. $ZnCl_2$ was added to a final zinc concentration of 50 nM and 10 µM (2.5 µM for liquid media), for the zinc-depleted and control media, respectively. Other cations were added back to their original concentrations: 0.9 mM Ca^{2+}, 0.25 µM Cu^{2+}, 1.2 µM Fe^{3+}, 7 mM K^{+}, 4.1 mM Mg^{2+}, 2.65 µM Mn^{2+}.

For growth curve analysis to assess the effect of zinc depletion and varying inositol concentrations on the *ino1Δ*, *zap1Δ* and wild-type strains, CYCD-inositol (0.5 % (w/v) yeast nitrogen base without amino acids and inositol (Formedium, UK), the rest as in CYCD) with inositol (Fluka, Switzerland) added to a final concentration of 20 mg/l (excess inositol concentration), 2 mg/l (control inositol concentration) or 0 mg/l (no inositol) was used.

To minimize the effect of vacuolar zinc storage on the results of all zinc depletion experiments, strains were first grown in Yeast Casamino Dextrose (YCD, prepared as CYCD with omitted chelation and addition of ions) before their transfer to zinc-deplete and control media. No intermediate media was used in the excess zinc experiments.

For excess zinc chemogenomics, YPD (1 % (w/v) yeast extract (Sigma, USA), 2 % (w/v) peptone (Sigma, USA), 2 % (w/v) glucose (Fluka, Germany), 2 % (w/v) agar (Sigma-Aldrich, USA)) with 4 mM or with no added $ZnCl_2$ was used in test and control media, respectively.

Growth fitness of *rim8Δ*, *rim9Δ*, *rim13Δ*, *rim20Δ*, *rim21Δ*, *rim101Δ*, *dfg16Δ*, *ygr122wΔ*, *stp22Δ*, *vps20Δ*, *vps25Δ*, *vps28Δ*, *vps36Δ*, *vps37Δ*, *snf7Δ*, *snf8Δ*, and the wild-type strain was assessed in YPD media containing 2 mM $ZnCl_2$, as well as control YPD media. Additionally, for growth curve analysis to test the combinatorial effects of pH and excess zinc, *rim9Δ*, *rim20Δ*, *rim101Δ, zap1Δ*, and the wild-type strain were grown in YPD media containing 150mM HEPES (4-(2-hydroxyethyl)-1-piperazineethanesulfonic acid; Serva, Germany) at pH 4 or 6 and a final 2 mM or 4 mM $ZnCl_2$ concentration. No $ZnCl_2$ was added in control media (buffered YPD).

To construct the query strain for synthetic genetic array (SGA) analysis, primers *IZH2*_up (GTTCCTTGAGCCAAATGTACTAAATTTCCCGTCGTTTTAATTATGAGCTTGCCTTGTCCCCGCCG) and *IZH2*_dn (TAAAACTACTTTCTATATAAATCCTACGTTTTTTCCAAATATCTATCGACACTGGATGGCGGCGT) were used to replace the *IZH2* gene of the parental strain AJY217 (S288c derivative; *MATα his3Δ leu2Δ ura3Δ met15Δ can1Δ::MFA1pr-HIS3 lyp1Δ*) with the NatMX resistance cassette from plasmid pAG25 (Euroscarf).

Zinc chemogenomics

To identify deletion strains sensitive to altered zinc concentrations (zinc-deplete or excess zinc conditions), plates from the yeast deletion collection were first pinned on test plates and then sequentially on control plates. To identify deletion strains resistant to altered zinc concentrations, plates were first pinned on control plates and then sequentially on test plates. Plates were incubated at 30°C for 48h (control plates of excess zinc screen), 72h (test plates in test-to-control direction of excess zinc screen; control plates of zinc-depletion screen), 96h (test plates of zinc-depletion screen, test plates in control-to-test direction of excess zinc screen). For both conditions the screen was done in triplicate. The relative growth fitness was determined as described in Mattiazzi *et al.*[86]. Higher confidence chemogenomic interactors were defined as those with relative growth fitness lower than (mean -2

standard deviations (SD)), while lower confidence interactors were defined as those with relative growth fitness between (mean -1SD) and (mean -2SD).

SGA analysis of the IZH2 gene

SGA analysis was carried out as described in Tong *et al.*[51]. For the identification of *IZH2* genetic interactors in altered zinc conditions, the obtained double mutants were pinned on zinc-depleted and excess zinc media as well as on corresponding control plates. The relative growth fitness of double mutants was calculated as described in Mattiazzi *et al.*[86]. Genetic interactors were identified as those that had relative growth fitness across biological replicates statistically significantly different (p-value < 0.05) from the average relative growth fitness of all strains.

Growth curve analysis

Growth curve measurements were done as described in Mattiazzi *et al.*[86]. Strains and media used are described above, with the exception of the reference strain where BY4741 strain was used.

Transcriptome analysis

DNA microarrays were used to determine the effect of the *IZH2* gene deletion on the yeast transcriptome. Gene expression in *izh2Δ* strain was compared to that of the control wild-type strain under zinc deplete (50 nM $ZnCl_2$) as well as under optimal zinc conditions (10 µM $ZnCl_2$).

Microarray post-processing, RNA sample preparation, cDNA synthesis, labeling, and DNA microarray hybridizations followed published procedures[87], with some modifications. For cDNA synthesis in the presence of amino-allyl dUTP 2µg mRNA were used. The test cDNA sample (*izh2*Δ strain) was labeled with Cy5 and the control sample (wild-type strain) with Cy3 fluorescent dye. For cleanup of cDNA synthesis and dye-coupling reactions QIAquick PCR purification kit (Qiagen, Chatsworth, CA, USA) was used. Microarray hybridizations were incubated at 65°C for 16 h. Microarrays were scanned with GenePix Personal 4100A microarray scanner (Axon Instruments, Union City, CA, USA) and analyzed using GenePix Pro 6.0 software (Axon Instruments). Cy5 and Cy3 median intensities were background-corrected and normalized using a regression correlation (NOMAD; http://ucsf-nomad.sourceforge.net/). Data was furher background-corrected and normalized using Bioconductor limma package[88], functions backgroundCorrect(method="normexp", offset=50), normalizeWithinArrays and normalizeBetweenArrays(method="Aquantile"). Differentially expressed genes were determined using Bioconductor limma package[88], functions lmFit and eBayes with default parameters. In Supplementary Table 3, we report p-values and FDR adjusted estimates for top 8000 differentially expressed genes (limma function toptable(number=8000, adjust="FDR")). We tested for differential expression between wild-type and *izh2Δ* deletion strain under zinc depletion and optimal zinc conditions, respectively (one replicate for each condition). This resulted in two lists of differentially expressed genes, one for each condition, which were used to investigate the specific function of Izh2 under the two conditions. To assess the role of Izh2 globally, microarray data from normal and limiting zinc were combined, and differential expression analysis was performed between the deletion strain and the wild-type.

All DNA microarray data is available from the ArrayExpress database (accession number: E-MEXP-3995).

Preparation of protein extracts

For Zrt1 induction, the indicated stains were grown to log-phase in YPD media and treated with EDTA (final concentration 1 mM) for the indicated times. To prepare whole cell extracts, 3 mL of cells were collected by centrifugation and the cell pellet was resuspended in 50 µL of Laemmli sample buffer[89] and heated for 5 minutes at 95^{o}C. For treatment with $ZnCl_2$, the indicated yeast strains were grown in minimal medium to mid-log phase. Cells were incubated for the indicated times in medium with or without $ZnCl_2$ (final concentration 2 mM), harvested by centrifugation, resuspended in homogenization

buffer (50 mM Tris [pH 7,6], 0.1 M KCl, 5 mM EDTA, 5 mM dithioerythritol, 20% [wt/vol] sucrose, protease inhibitor cocktail [Roche]) and lysed by vortexing with glass beads. The lysate was centrifuged for 5 min at 500 *g* to remove insoluble material. The crude extract was separated into soluble and particulate fractions by centrifugation for 30 min at 16,000 *g* at 4°C. The particulate fraction was resuspended directly in Laemmli sample buffer.

Immunoblots

Proteins were separated by sodium dodecyl sulfate-polyacrylamide gel electrophoresis, transferred to nitrocellulose membranes, and immunoblotted with a monoclonal anti-GFP antibody (Roche Diagnostics GmbH, Mannheim, Germany). Immunoreactive bands were visualized using the ECL-Plus chemiluminescence system and horseradish peroxidase-conjugated secondary antibodies (Amersham Biosciences UK Ltd., England). Western blots were quantified using the Image Gauge software v. 4.0. Zrt1-GFP signals were normalized using the Direct Blue 71 (Sigma) staining of the membrane.

Preparation of Yeast RNA

The indicated strains were grown in YPD medium to mid-log phase and treated with EDTA (final concentration 1 mM) for the indicated times. One hundred mL of cells were harvested by centrifugation. Cell pellets were resuspended in 150 µL TCES buffer (0.2 M NaCl, 0.2 M Tris-HCl [pH 8], 0.05 M EDTA, sodium dodecyl sulfate 2%) and 500 µL of glass beads (0.45-0.50 mm diameter) were added to the cell suspension. Immediately following addition of 150 µL of phenol/chloroform/isoamyl alcohol mixture (25:24:1 [v/v/v]), cells were broken by vigorous vortexing. After addition of 200 µL TCES buffer and a brief centrifugation, the supernatant was transferred to a fresh tube and one volume of chloroform/isoamyl alcohol (24/1) was added. After vortexing, the mixture was centrifuged for 3 minutes. The RNA contained in the upper phase was precipitated by adding 2 volumes of ethanol, collected by centrifugation, washed with 70% ethanol, dried and resuspended in 30 µL of sterile Milli-Q water.

Northern blot analysis

Twenty µg of RNA per lane were separated in formaldehyde gels and blotted onto nylon membranes (Hybond-N, Amersham). Probes containing PCR-derived fragments of GFP (bp 43-490) or *ACT1* (bp 518-1182) were radioactively labeled using the High Prime kit (Roche, France) following manufacturer's instructions. Radioactively labeled probes were hybridized in PSE buffer (300 mM NaH_2PO_4/Na_2HPO_4 pH 7.2, 7% SDS, 1 mM EDTA) for 12 hours at 65°C. Membranes were washed twice with 4x SSC/0.1% SDS and once with 0.4x SSC/0.1% SDS for 10 minutes at 65°C. Signals were quantified using a Fujifilm BAS-1500 phosphoimager. Data are expressed as the ratio of GFP/*ACT1* signal in each strain and condition.

Intracellular zinc concentration measurements

Intracellular zinc concentrations were determined by flame atomic absorption spectrometry on a Varian SpectrAA 110 spectrometer (Mulgrove, Victoria, Australia) in *rim101*Δ, *rim8*Δ, *dfg16*Δ, *zrt1*Δ, *zap1*Δ and corresponding wild type reference (BY4741) strains. The cultures were grown in YPD (pH 5.4) media under normal and elevated environmental zinc levels (4 mM) from the initial OD_{600} of approximately 0.2 till OD_{600} of 0.8-1.0. Cells (100 mL of culture) were then collected by centrifugation, washed twice with 10 mL cold 1 mM EDTA, once with 10 mL cold miliQ, flash frozen in liquid nitrogen and stored at -80°C.
For intracellular zinc measurements the collected cells were digested in a mixture of 200 µL 30 % H_2O_2 and 200 µL 65 % HNO_3 for approximately 42 h at 80°C to obtain a clear solution. Before determination by FASS samples were diluted with miliQ water to 50 mL.

Acknowledgments

This work was supported by grant P1-0207 from the Slovenian Research Agency. M.M.U. was supported by the Young Investigator fellowship scheme from the Slovenian Research Agency. Work done in the group of L.Y. was funded by grant BFU2011-30197-C03-03 from the Spanish Ministry of Science and Innovation (Madrid, Spain). C.P. was supported by a pre-doctoral fellowship from the Spanish Research Council.

References

1. L. A. Finney and T. V. O'Halloran, *Science*, 2003, **300**, 931-936.
2. D. J. Eide, *Biochim Biophys Acta*, 2006, **1763**, 711-722.
3. C. Andreini, L. Banci, I. Bertini and A. Rosato, *J Proteome Res*, 2006, **5**, 196-201.
4. M. M. Mihaylova and R. J. Shaw, *Trends Endocrinol Metab*, 2013, **24**, 48-57.
5. N. Sadli, M. L. Ackland, D. De Mel, A. J. Sinclair and C. Suphioglu, *Cell Physiol Biochem*, 2012, **29**, 87-98.
6. T. M. Bray and W. J. Bettger, *Free Radic Biol Med*, 1990, **8**, 281-291.
7. G. M. Carman and G. S. Han, *Biochim Biophys Acta*, 2007, **1771**, 322-330.
8. W. M. Iwanyshyn, G. S. Han and G. M. Carman, *J Biol Chem*, 2004, **279**, 21976-21983.
9. A. B. Chausmer, *J Am Coll Nutr*, 1998, **17**, 109-115.
10. S. L. Kelleher, N. H. McCormick, V. Velasquez and V. Lopez, *Adv Nutr*, 2011, **2**, 101-111.
11. G. Dodson and D. Steiner, *Curr Opin Struct Biol*, 1998, **8**, 189-194.
12. M. E. Trujillo and P. E. Scherer, *J Intern Med*, 2005, **257**, 167-175.
13. F. Vasseur, *Pharmacol Res*, 2006, **53**, 478-481.
14. T. Kadowaki, T. Yamauchi, N. Kubota, K. Hara, K. Ueki and K. Tobe, *J Clin Invest*, 2006, **116**, 1784-1792.
15. I. V. Karpichev, L. Cornivelli and G. M. Small, *J Biol Chem*, 2002, **277**, 19609-19617.
16. T. J. Lyons, N. Y. Villa, L. M. Regalla, B. R. Kupchak, A. Vagstad and D. J. Eide, *Proc Natl Acad Sci U S A*, 2004, **101**, 5506-5511.
17. Y. Jiang, M. J. Vasconcelles, S. Wretzel, A. Light, C. E. Martin and M. A. Goldberg, *Mol Cell Biol*, 2001, **21**, 6161-6169.
18. M. L. Narasimhan, M. A. Coca, J. Jin, T. Yamauchi, Y. Ito, T. Kadowaki, K. K. Kim, J. M. Pardo, B. Damsz, P. M. Hasegawa, D. J. Yun and R. A. Bressan, *Mol Cell*, 2005, **17**, 171-180.
19. B. R. Kupchak, I. Garitaonandia, N. Y. Villa, M. B. Mullen, M. G. Weaver, L. M. Regalla, E. A. Kendall and T. J. Lyons, *Biochim Biophys Acta*, 2007, **1773**, 1124-1132.
20. L. Zhang, Y. Zhang, Y. Zhou, S. An and J. Cheng, *J Antimicrob Chemother*, 2002, **49**, 905-915.
21. G. Giaever, A. M. Chu, L. Ni, C. Connelly, L. Riles, S. Veronneau, S. Dow, A. Lucau-Danila, K. Anderson, B. Andre, A. P. Arkin, A. Astromoff, M. El-Bakkoury, R. Bangham, R. Benito, S. Brachat, S. Campanaro, M. Curtiss, K. Davis, A. Deutschbauer, K. D. Entian, P. Flaherty, F. Foury, D. J. Garfinkel, M. Gerstein, D. Gotte, U. Guldener, J. H. Hegemann, S. Hempel, Z. Herman, D. F. Jaramillo, D. E. Kelly, S. L. Kelly, P. Kotter, D. LaBonte, D. C. Lamb, N. Lan, H. Liang, H. Liao, L. Liu, C. Luo, M. Lussier, R. Mao, P. Menard, S. L. Ooi, J. L. Revuelta, C. J. Roberts, M. Rose, P. Ross-Macdonald, B. Scherens, G. Schimmack, B. Shafer, D. D. Shoemaker, S. Sookhai-Mahadeo, R. K. Storms, J. N. Strathern, G. Valle, M. Voet, G. Volckaert, C. Y. Wang, T. R. Ward, J. Wilhelmy, E. A. Winzeler, Y. Yang, G. Yen, E. Youngman, K. Yu, H. Bussey, J. D. Boeke, M. Snyder, P. Philippsen, R. W. Davis and M. Johnston, *Nature*, 2002, **418**, 387-391.
22. C. W. MacDiarmid, L. A. Gaither and D. Eide, *EMBO J*, 2000, **19**, 2845-2855.
23. H. Zhao and D. Eide, *Proc Natl Acad Sci U S A*, 1996, **93**, 2454-2458.
24. M. North, J. Steffen, A. V. Loguinov, G. R. Zimmerman, C. D. Vulpe and D. J. Eide, *PLoS Genet*, 2012, **8**, e1002699.

25. C. Y. Wu, A. J. Bird, D. R. Winge and D. J. Eide, *J Biol Chem*, 2007, **282**, 2184-2195.
26. D. S. Yuan, *Genetics*, 2000, **156**, 45-58.
27. H. Zhao and D. J. Eide, *Mol Cell Biol*, 1997, **17**, 5044-5052.
28. L. Li and J. Kaplan, *J Biol Chem*, 1997, **272**, 28485-28493.
29. M. A. Pagani, A. Casamayor, R. Serrano, S. Atrian and J. Arino, *Mol Microbiol*, 2007, **65**, 521-537.
30. A. Harington, C. J. Herbert, B. Tung, G. S. Getz and P. P. Slonimski, *Mol Microbiol*, 1993, **9**, 545-555.
31. A. Harington, E. Schwarz, P. P. Slonimski and C. J. Herbert, *EMBO J*, 1994, **13**, 5531-5538.
32. T. Shintani, K. Suzuki, Y. Kamada, T. Noda and Y. Ohsumi, *J Biol Chem*, 2001, **276**, 30452-30460.
33. C. W. Wang, J. Kim, W. P. Huang, H. Abeliovich, P. E. Stromhaug, W. A. Dunn, Jr. and D. J. Klionsky, *J Biol Chem*, 2001, **276**, 30442-30451.
34. J. Ambroziak and S. A. Henry, *J Biol Chem*, 1994, **269**, 15344-15349.
35. M. L. Greenberg and J. M. Lopes, *Microbiol Rev*, 1996, **60**, 1-20.
36. A. Kamizono, M. Nishizawa, Y. Teranishi, K. Murata and A. Kimura, *Mol Gen Genet*, 1989, **219**, 161-167.
37. M. E. Hillenmeyer, E. Fung, J. Wildenhain, S. E. Pierce, S. Hoon, W. Lee, M. Proctor, R. P. St Onge, M. Tyers, D. Koller, R. B. Altman, R. W. Davis, C. Nislow and G. Giaever, *Science*, 2008, **320**, 362-365.
38. C. W. MacDiarmid, M. A. Milanick and D. J. Eide, *J Biol Chem*, 2002, **277**, 39187-39194.
39. D. Hoepfner, S. B. Helliwell, H. Sadlish, S. Schuierer, I. Filipuzzi, S. Brachat, B. Bhullar, U. Plikat, Y. Abraham, M. Altorfer, T. Aust, L. Baeriswyl, R. Cerino, L. Chang, D. Estoppey, J. Eichenberger, M. Frederiksen, N. Hartmann, A. Hohendahl, B. Knapp, P. Krastel, N. Melin, F. Nigsch, E. J. Oakeley, V. Petitjean, F. Petersen, R. Riedl, E. K. Schmitt, F. Staedtler, C. Studer, J. A. Tallarico, S. Wetzel, M. C. Fishman, J. A. Porter and N. R. Movva, *Microbiol Res*, 2014, **169**, 107-120.
40. N. Umeda, T. Suzuki, M. Yukawa, Y. Ohya, H. Shindo and K. Watanabe, *J Biol Chem*, 2005, **280**, 1613-1624.
41. A. Lucau-Danila, T. Delaveau, G. Lelandais, F. Devaux and C. Jacq, *J Biol Chem*, 2003, **278**, 52641-52650.
42. E. Lamping, J. Luckl, F. Paltauf, S. A. Henry and S. D. Kohlwein, *Genetics*, 1994, **137**, 55-65.
43. C. Wagner, M. Dietz, J. Wittmann, A. Albrecht and H. J. Schuller, *Mol Microbiol*, 2001, **41**, 155-166.
44. J. H. Boysen and A. P. Mitchell, *Mol Biol Cell*, 2006, **17**, 1344-1353.
45. K. Rothfels, J. C. Tanny, E. Molnar, H. Friesen, C. Commisso and J. Segall, *Mol Cell Biol*, 2005, **25**, 6772-6788.
46. K. J. Barwell, J. H. Boysen, W. Xu and A. P. Mitchell, *Eukaryot Cell*, 2005, **4**, 890-899.
47. K. Selvig and J. A. Alspaugh, *Mycobiology*, 2011, **39**, 249-256.
48. T. M. Lamb and A. P. Mitchell, *Mol Cell Biol*, 2003, **23**, 677-686.
49. W. Xu and A. P. Mitchell, *J Bacteriol*, 2001, **183**, 6917-6923.
50. K. Obara, H. Yamamoto and A. Kihara, *J Biol Chem*, 2012, **287**, 38473-38481.
51. A. H. Tong, M. Evangelista, A. B. Parsons, H. Xu, G. D. Bader, N. Page, M. Robinson, S. Raghibizadeh, C. W. Hogue, H. Bussey, B. Andrews, M. Tyers and C. Boone, *Science*, 2001, **294**, 2364-2368.
52. M. F. Manolson, B. Wu, D. Proteau, B. E. Taillon, B. T. Roberts, M. A. Hoyt and E. W. Jones, *J Biol Chem*, 1994, **269**, 14064-14074.
53. J. H. Seol, A. Shevchenko and R. J. Deshaies, *Nat Cell Biol*, 2001, **3**, 384-391.
54. A. M. Smardon, M. Tarsio and P. M. Kane, *J Biol Chem*, 2002, **277**, 13831-13839.
55. T. Nakamura, S. Takahashi, H. Takagi and J. Shima, *FEMS Yeast Res*, 2010, **10**, 259-269.

56. M. Costanzo, A. Baryshnikova, J. Bellay, Y. Kim, E. D. Spear, C. S. Sevier, H. Ding, J. L. Koh, K. Toufighi, S. Mostafavi, J. Prinz, R. P. St Onge, B. VanderSluis, T. Makhnevych, F. J. Vizeacoumar, S. Alizadeh, S. Bahr, R. L. Brost, Y. Chen, M. Cokol, R. Deshpande, Z. Li, Z. Y. Lin, W. Liang, M. Marback, J. Paw, B. J. San Luis, E. Shuteriqi, A. H. Tong, N. van Dyk, I. M. Wallace, J. A. Whitney, M. T. Weirauch, G. Zhong, H. Zhu, W. A. Houry, M. Brudno, S. Ragibizadeh, B. Papp, C. Pal, F. P. Roth, G. Giaever, C. Nislow, O. G. Troyanskaya, H. Bussey, G. D. Bader, A. C. Gingras, Q. D. Morris, P. M. Kim, C. A. Kaiser, C. L. Myers, B. J. Andrews and C. Boone, *Science*, 2010, **327**, 425-431.
57. F. Ricarte, R. Menjivar, S. Chhun, T. Soreta, L. Oliveira, T. Hsueh, M. Serranilla and E. Gharakhanian, *PLoS One*, 2011, **6**, e23696.
58. N. Belgareh-Touze, S. Avaro, Y. Rouille, B. Hoflack and R. Haguenauer-Tsapis, *Mol Biol Cell*, 2002, **13**, 1694-1708.
59. A. Cohen, N. Perzov, H. Nelson and N. Nelson, *J Biol Chem*, 1999, **274**, 26885-26893.
60. N. Ogawa, J. DeRisi and P. O. Brown, *Mol Biol Cell*, 2000, **11**, 4309-4321.
61. N. G. Tsvetanova, D. M. Klass, J. Salzman and P. O. Brown, *PLoS One*, 2010, **5**.
62. V. J. Higgins, P. J. Rogers and I. W. Dawes, *Appl Environ Microbiol*, 2003, **69**, 7535-7540.
63. O. Protchenko, T. Ferea, J. Rashford, J. Tiedeman, P. O. Brown, D. Botstein and C. C. Philpott, *J Biol Chem*, 2001, **276**, 49244-49250.
64. L. Shi and B. P. Tu, *Proc Natl Acad Sci U S A*, 2013, **110**, 7318-7323.
65. J. S. Flick and J. Thorner, *Genetics*, 1998, **148**, 33-47.
66. R. Ghillebert, E. Swinnen, P. De Snijder, B. Smets and J. Winderickx, *Biochem J*, 2011, **434**, 243-251.
67. T. R. Hughes, M. J. Marton, A. R. Jones, C. J. Roberts, R. Stoughton, C. D. Armour, H. A. Bennett, E. Coffey, H. Dai, Y. D. He, M. J. Kidd, A. M. King, M. R. Meyer, D. Slade, P. Y. Lum, S. B. Stepaniants, D. D. Shoemaker, D. Gachotte, K. Chakraburtty, J. Simon, M. Bard and S. H. Friend, *Cell*, 2000, **102**, 109-126.
68. C. von Mering, R. Krause, B. Snel, M. Cornell, S. G. Oliver, S. Fields and P. Bork, *Nature*, 2002, **417**, 399-403.
69. J. Lamb, E. D. Crawford, D. Peck, J. W. Modell, I. C. Blat, M. J. Wrobel, J. Lerner, J. P. Brunet, A. Subramanian, K. N. Ross, M. Reich, H. Hieronymus, G. Wei, S. A. Armstrong, S. J. Haggarty, P. A. Clemons, R. Wei, S. A. Carr, E. S. Lander and T. R. Golub, *Science*, 2006, **313**, 1929-1935.
70. T. J. Lyons, A. P. Gasch, L. A. Gaither, D. Botstein, P. O. Brown and D. J. Eide, *Proc Natl Acad Sci U S A*, 2000, **97**, 7957-7962.
71. J. J. Wyrick, F. C. Holstege, E. G. Jennings, H. C. Causton, D. Shore, M. Grunstein, E. S. Lander and R. A. Young, *Nature*, 1999, **402**, 418-421.
72. S. A. Henry, S. D. Kohlwein and G. M. Carman, *Genetics*, 2012, **190**, 317-349.
73. Z. Hu, P. J. Killion and V. R. Iyer, *Nat Genet*, 2007, **39**, 683-687.
74. H. Zhao and D. Eide, *J Biol Chem*, 1996, **271**, 23203-23210.
75. B. P. Young, J. J. Shin, R. Orij, J. T. Chao, S. C. Li, X. L. Guan, A. Khong, E. Jan, M. R. Wenk, W. A. Prinz, G. J. Smits and C. J. Loewen, *Science*, 2010, **329**, 1085-1088.
76. J. Arino, J. Ramos and H. Sychrova, *Microbiol Mol Biol Rev*, 2010, **74**, 95-120.
77. T. M. Lamb, W. Xu, A. Diamond and A. P. Mitchell, *J Biol Chem*, 2001, **276**, 1850-1856.
78. S. Berthelet, J. Usher, K. Shulist, A. Hamza, N. Maltez, A. Johnston, Y. Fong, L. J. Harris and K. Baetz, *Genetics*, 2010, **185**, 1111-1128.
79. A. Ferrari, E. Fiorino, M. Giudici, F. Gilardi, A. Galmozzi, N. Mitro, G. Cermenati, C. Godio, D. Caruso, E. De Fabiani and M. Crestani, *Mol Membr Biol*, 2012, **29**, 257-266.
80. M. J. Hickman, D. Spatt and F. Winston, *Genetics*, 2011, **188**, 325-338.
81. S. A. Jesch, P. Liu, X. Zhao, M. T. Wells and S. A. Henry, *J Biol Chem*, 2006, **281**, 24070-24083.

82. B. E. Bernstein, J. K. Tong and S. L. Schreiber, *Proc Natl Acad Sci U S A*, 2000, **97**, 13708-13713.
83. C. J. Millard, P. J. Watson, I. Celardo, Y. Gordiyenko, S. M. Cowley, C. V. Robinson, L. Fairall and J. W. Schwabe, *Mol Cell*, 2013, **51**, 57-67.
84. C. Ye, W. M. Bandara and M. L. Greenberg, *J Biol Chem*, 2013, **288**, 24898-24908.
85. M. S. Longtine, A. McKenzie, 3rd, D. J. Demarini, N. G. Shah, A. Wach, A. Brachat, P. Philippsen and J. R. Pringle, *Yeast*, 1998, **14**, 953-961.
86. M. Mattiazzi, A. Jambhekar, P. Kaferle, J. L. Derisi, I. Krizaj and U. Petrovic, *Mol Genet Genomics*, 2010, **283**, 519-530.
87. J. L. DeRisi, V. R. Iyer and P. O. Brown, *Science*, 1997, **278**, 680-686.
88. M. E. Ritchie, B. Phipson, D. Wu, Y. Hu, C. W. Law, W. Shi and G. K. Smyth, *Nucleic Acids Res*, 2015, **43**, e47.
89. D. W. Cleveland, S. G. Fischer, M. W. Kirschner and U. K. Laemmli, *J Biol Chem*, 1977, **252**, 1102-1106.

Figure 1: **Growth curves under conditions of different pH and elevated zinc levels of selected strains.** A-C) Growth curves of mutants in the Rim101 pathway components at elevated Zn concentrations (2 mM and 4 mM) at pH 4 and pH 6. The control Zn concentration was 2.5 µM. D) Growth curves of the *zap1*Δ mutant at elevated Zn concentrations (2 mM and 4 mM) at pH 4 and pH 6. The control Zn concentration was 2.5 µM. WT – reference strain.

Figure 2: **Numbers of genes identified in *IZH2* genetic interaction screens and their overlap with Zn chemogenomic screens.** A) Number of genes in genetic interaction with *IZH2* at different Zn concentrations: Zn depletion – 50 nM, normal Zn – 10 µM, Zn overload – 4 mM. B) Overlap of genes in genetic interaction with *IZH2* and genes whose mutations render the yeast cell sensitive or resistant to depleted (50 nM) or excess (4 mM) zinc.

Figure 3: **Growth curves of reference strain, *zap1*Δ and *ino1*Δ cells at different inositol and zinc concentrations**. A) No inositol in the medium. B) Concentration of inositol in the medium 2 mg/mL. B) Concentration of inositol in the medium 20 mg/mL. D – depleted Zn (50 nM); C – control Zn concentration (2.5 µM); WT – reference strain.

Figure 4: **Zrt1 protein and mRNA expression levels in Rim101 pathway mutants**. A) Zrt1 protein levels in response to zinc overload (final concentration 2 mM $ZnCl_2$). B) Zrt1 protein levels in response to zinc depletion. Strains were treated for the indicated time (in hours) with 1 mM EDTA. In both cases the amount of Zrt1-GFP protein was analyzed by immunoblotting using a specific GFP antibody. Direct Blue staining of the membrane is shown in the lower panels as a loading control with relative intensity of the normalized signal indicated below each lane. Similar results were observed for 2 independent transformants. C) Zrt1 mRNA levels in response to zinc depletion. The amount of *ZRT1-GFP* transcript was analyzed by northern blot using a specific GFP probe. The *ACT1* gene was used to normalize *ZRT1* expression levels. Data are expressed in arbitrary units. Shown are average values and standard deviations of 3 independent replicates. * p-value < 0.05. WT – reference strain.

Figure 5: **Flame atomic absorption spectrometry analysis of total intracellular zinc concentrations.** A) Cells were grown in rich (YPD) medium under normal extracellular zinc concentration (10 µM). B) Cells were grown in rich (YPD) medium under elevated extracellular zinc concentration (4 mM). C) Ratio of intracellular zinc concentration between cells grown under elevated and normal extracellular zinc concentrations. Error bars represent standard deviation from two independent measurements. *** p-value < 0.001, ** p-value < 0.01. WT – reference strain.

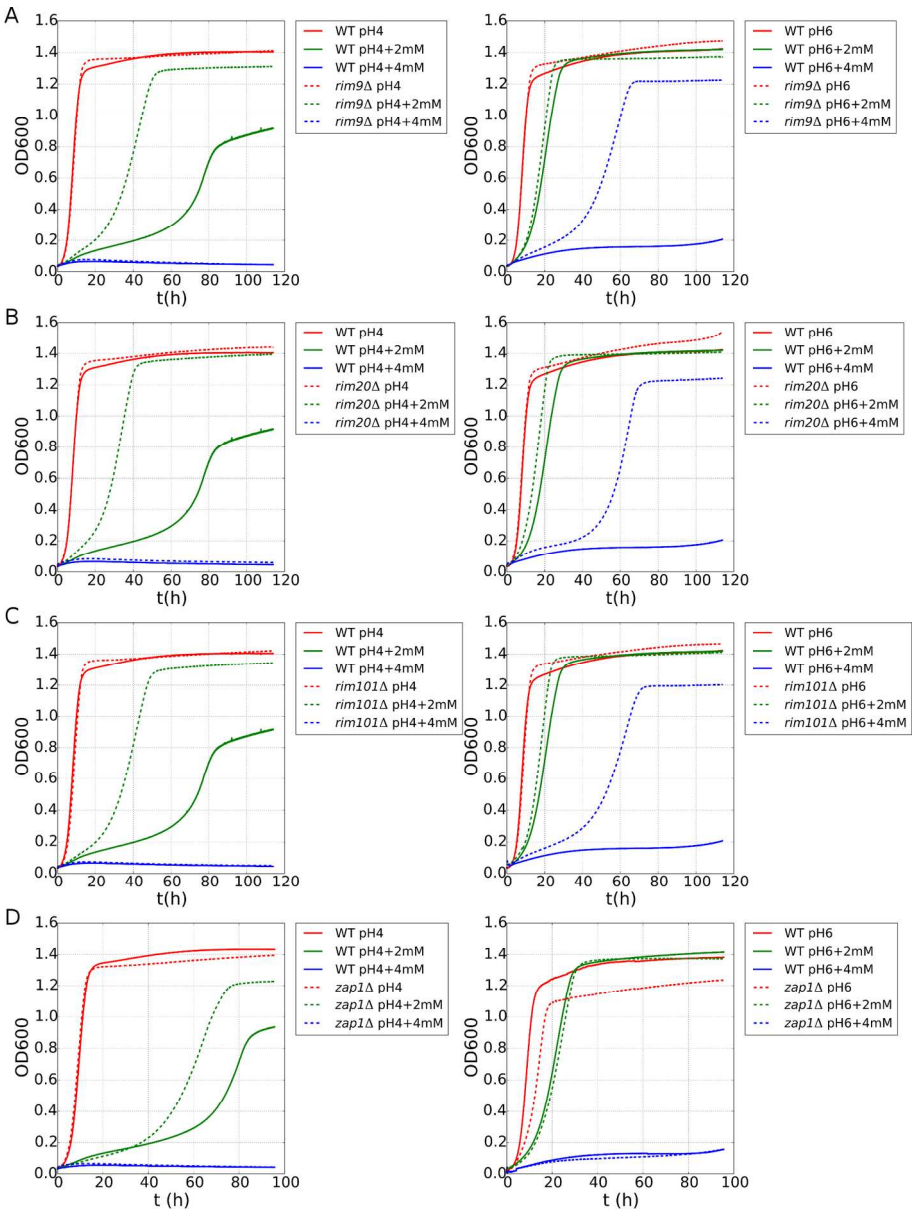

Growth curves under conditions of different pH and elevated zinc levels of selected strains. A-C) Growth curves of mutants in the Rim101 pathway components at elevated Zn concentrations (2 mM and 4 mM) at pH 4 and pH 6. The control Zn concentration was 2.5 μM. D) Growth curves of the zap1Δ mutant at elevated Zn concentrations (2 mM and 4 mM) at pH 4 and pH 6. The control Zn concentration was 2.5 μM. WT – reference strain.
170x224mm (300 x 300 DPI)

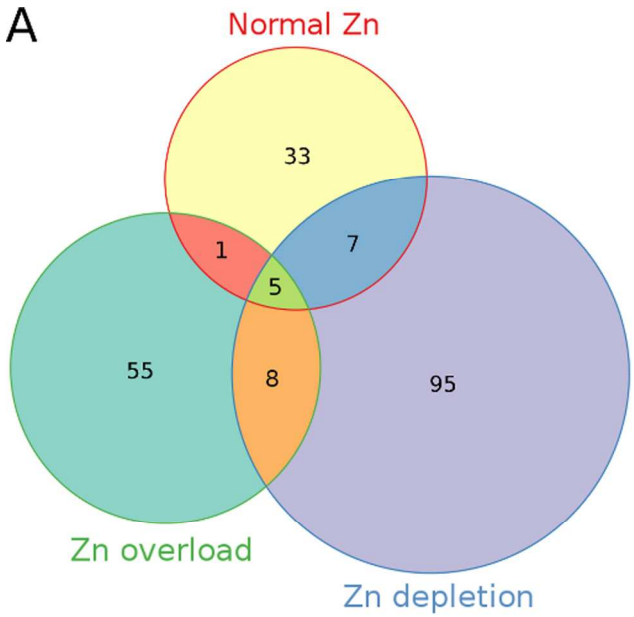

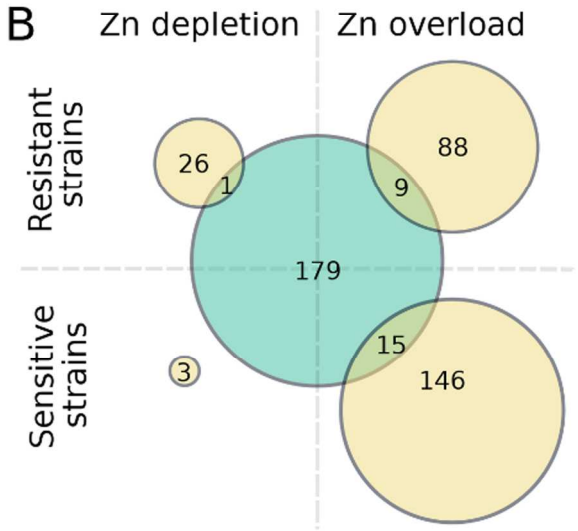

Numbers of genes identified in IZH2 genetic interaction screens and their overlap with Zn chemogenomic screens. A) Number of genes in genetic interaction with IZH2 at different Zn concentrations: Zn depletion – 50 nM, normal Zn – 10 μM, Zn overload – 4 mM. B) Overlap of genes in genetic interaction with IZH2 and genes whose mutations render the yeast cell sensitive or resistant to depleted (50 nM) or excess (4 mM) zinc.
80x153mm (300 x 300 DPI)

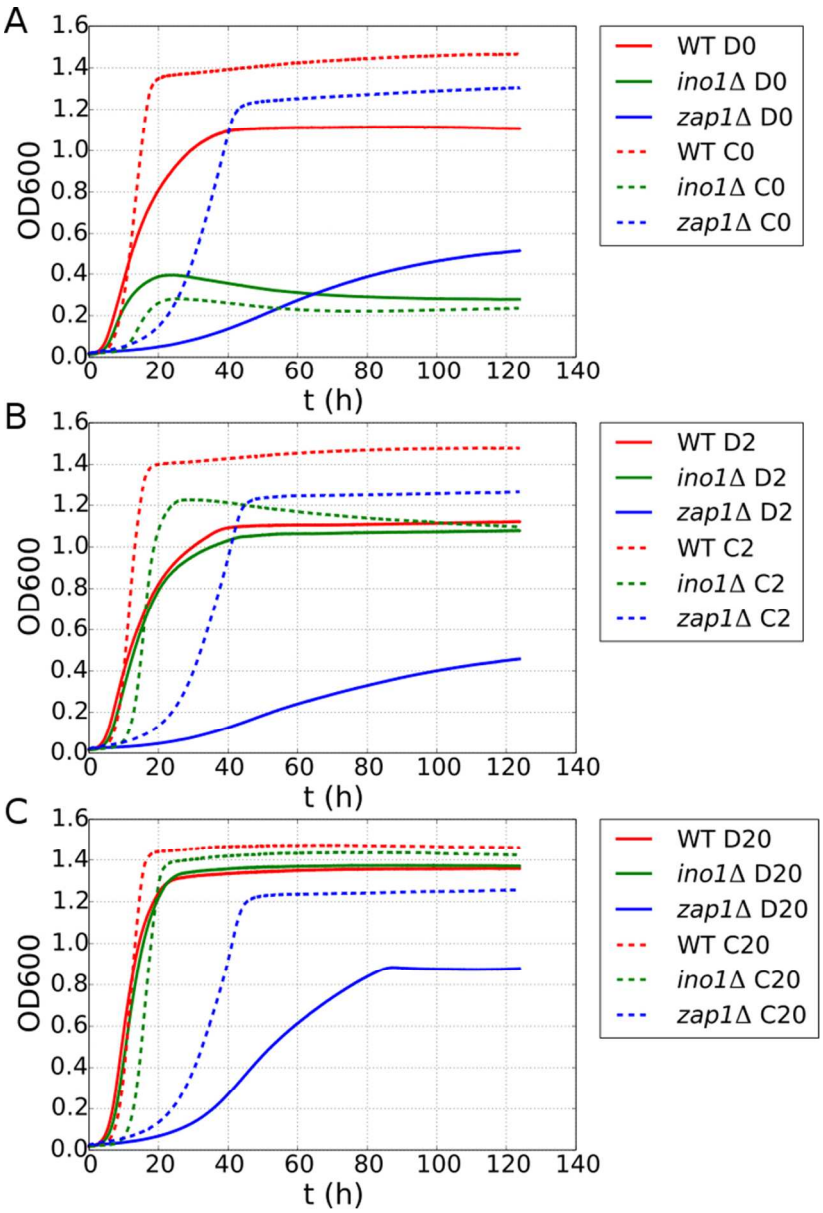

Growth curves of reference strain, zap1Δ and ino1Δ cells at different inositol and zinc concentrations. A) No inositol in the medium. B) Concentration of inositol in the medium 2 mg/mL. B) Concentration of inositol in the medium 20 mg/mL. D – depleted Zn (50 nM); C – control Zn concentration (2.5 μM); WT – reference strain.
80x117mm (300 x 300 DPI)

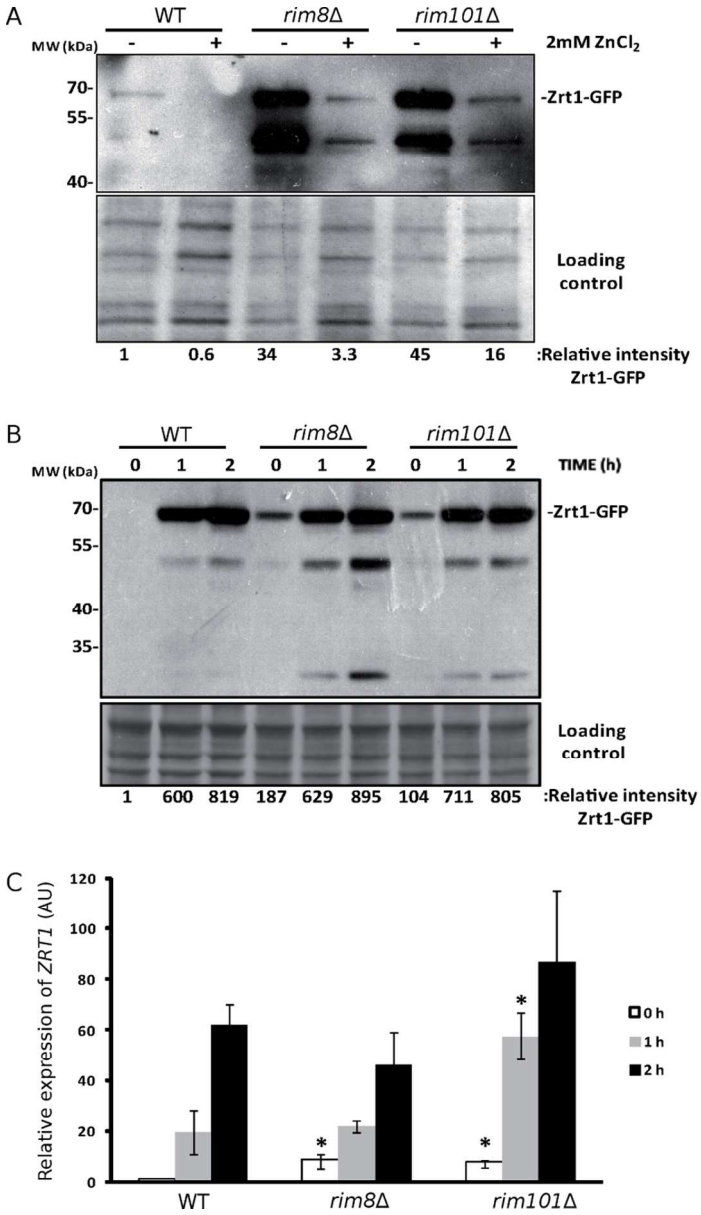

Zrt1 protein and mRNA expression levels in Rim101 pathway mutants. A) Zrt1 protein levels in response to zinc overload (final concentration 2 mM $ZnCl_2$). B) Zrt1 protein levels in response to zinc depletion. Strains were treated for the indicated time (in hours) with 1 mM EDTA. In both cases the amount of Zrt1-GFP protein was analyzed by immunoblotting using a specific GFP antibody. Direct Blue staining of the membrane is shown in the lower panels as a loading control with relative intensity of the normalized signal indicated below each lane. Similar results were observed for 2 independent transformants. C) Zrt1 mRNA levels in response to zinc depletion. The amount of *ZRT1-GFP* transcript was analyzed by northern blot using a specific GFP probe. The *ACT1* gene was used to normalize *ZRT1* expression levels. Data are expressed in arbitrary units. Shown are average values and standard deviations of 3 independent replicates. * p-value < 0.05. WT – reference strain.
85x147mm (300 x 300 DPI)

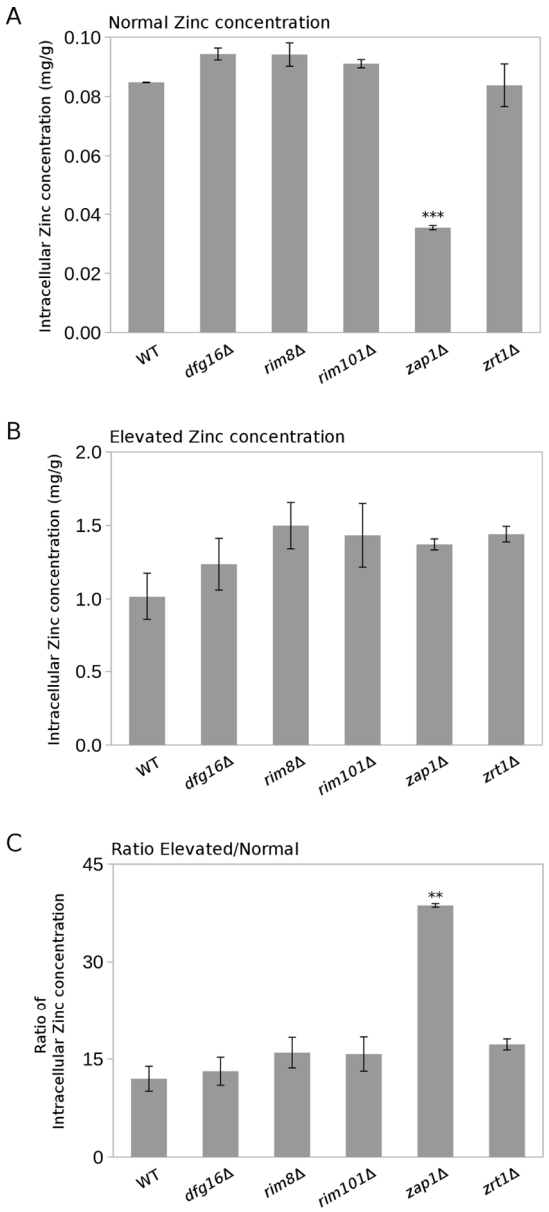

Flame atomic absorption spectrometry analysis of total intracellular zinc concentrations. A) Cells were grown in rich (YPD) medium under normal extracellular zinc concentration (10 μM). B) Cells were grown in rich (YPD) medium under elevated extracellular zinc concentration (4 mM). C) Ratio of intracellular zinc concentration between cells grown under elevated and normal extracellular zinc concentrations. Error bars represent standard deviation from two independent measurements. *** p-value < 0.001, ** p-value < 0.01. WT – reference strain.
82x183mm (300 x 300 DPI)